GEOPHYSICS, VOL. 37, NO. 5 (OCTOBER 1972), P. 862-878, 18 FIGS.

8-HZ TELLURIC AND MAGNETOTELLURIC PROSPECTING†

J. A. SLANKIS*, W. M. TELFORD‡, AND A. BECKER**

Telluric and magnetotelluric surveys utilizing natural 8-hz electromagnetic fields have detected resistivity variations associated with some proven sulfide deposits. From an operational point of view the telluric method is preferred to magnetotellurics. Either method, however, can detect a conducting dike, providing that its width is greater than its depth of burial.

For surveys where the telluric field is measured in a direction perpendicular to the strike of the conductor, theoretical profiles derived from two-dimensional conductivity structures agree well with the field results. For this polarization, it is thus possible to use a general model as an aid to the interpretation of survey data.

INTRODUCTION

Geophysical techniques that utilize natural electromagnetic fields include AFMAG and the magnetotelluric and telluric methods. All of these will detect lateral changes in resistivity, but only magnetotellurics can be used to determine resistivity changes with depth. The AFMAG method has been used both for mineral exploration and geologic mapping (Collett and Bell, 1971), while magnetotelluric measurements have been employed for resistivity depth sounding in both petroleum exploration and geologic mapping (Strangway and Vozoff, 1970). The telluric method has been used less than the other techniques, and only a few papers describing its application to geologic mapping (Neuenschwander and Metcalf, 1942; Dahlberg, 1945; Boissonnas and Leonardon, 1948; Berdichevskiy, 1960; Srivastava et al, 1963) have been published.

This paper describes some results obtained during a joint project of McGill University and the Geological Survey of Canada to evaluate the usefulness of subaudio-frequency telluric and, to a lesser extent, magnetotelluric measurements for mineral exploration. The primary purpose of this project was to design, construct, and test equipment suitable for field surveying. After the field surveys showed the methods to be useful, the field results were compared to theoretical profiles computed, using the transmission surface analogy developed by Madden and his coworkers (Madden and Thompson, 1965; Madden and Swift, 1969; Swift, 1971). Because the theoretical results proved to be of value in interpreting field data, the potential of the methods was investigated further on the basis of the theoretical models.

GENERAL PRINCIPLES

In the magnetotelluric method the resistivity of a homogeneous half-space is determined from the following relation between the horizontal magnetic and electric fields at the earth's surface (Cagniard, 1953):

$$E = \sqrt{5f\rho}\, H,$$

where

ρ = resistivity of the ground (ohm-m),
f = frequency of signal (hz),
E = magnitude of horizontal electric field (mv/km), and

† Presented at the 39th Annual International SEG Meeting, September 17, 1969 Calgary, Alberta. Manuscript received by the Editor July 26, 1971; revised manuscript received November 1, 1971.

* Texas Gulf, Inc., Toronto, Ontario.

‡ McGill University, Montreal, Quebec.

** Geological Survey of Canada, Ottawa, Ontario.

© 1972 by the Society of Exploration Geophysicists. All rights reserved.

H = magnitude of orthogonal horizontal magnetic field (gammas).

If, however, the ground consists of horizontal layers, or if there are nearby lateral changes in conductivity, the above relation serves as a definition of an "apparent" resistivity which will be a function of the frequency at which the measurement is made and of the resistivity geometry of the subsurface.

In the particular case where all resistivity features are assumed to be two-dimensional (i.e., of infinite strike extent), the electric and magnetic fields can be resolved into components normal and parallel to the strike of a resistivity discontinuity. Therefore, there are two pairs of orthogonal fields ($E_\perp$ and $H_\parallel$, and $E_\parallel$ and $H_\perp$, Figure 1).

In the $E_\perp$ case, the magnetic field ($H_\parallel$) is invariant (Weaver, 1963), and lateral changes in the resistivity of the ground are reflected only in variations of the electric fields. If $E_\perp$ and $H_\parallel$ are measured simultaneously at two points, then

$$E_\perp^{(1)}/E_\perp^{(2)} = (\rho^{(1)}/\rho^{(2)})^{1/2}.$$

Since $H^{(1)}{}_\parallel = H^{(2)}{}_\parallel$, the ratio of telluric field strengths is proportional to the square root of apparent resistivities at the two locations. Therefore, for this polarization, if the apparent resistivity is known at one location, an apparent-resistivity profile can be obtained by measuring variations in the telluric field strength. This was the basis for most of the telluric measurements made during this work.

In the $E_\parallel$ case, both $E_\parallel$ and $H_\perp$ vary across a conductivity interface, and magnetotelluric measurements are necessary to obtain an apparent-resistivity profile.

EQUIPMENT

In order to make the equipment simple and completely portable, measurements were made at a single frequency using the 8-hz thunderstorm signal propagated in the first Schumann resonance mode. The choice of this low frequency was attractive because of its rather large and constant amplitude (Galejs, 1964; Shand, 1966) and the probability of obtaining a considerable depth of penetration.

The measuring equipment consists of two identical microvoltmeters sharply tuned at 8 hz. Figure 2 is a block diagram of the amplifiers. Only one unit includes a bandpass compensator having the same frequency characteristics as the magnetic sensing system. Thus, with switch SW1 in the position shown, the two amplifiers could be used for telluric surveys. For magnetotelluric measurements, the set with the extra filter section was used to measure the telluric field.

Figure 3 shows the frequency responses of the amplifiers in the telluric and magnetotelluric modes. These have been superimposed on a

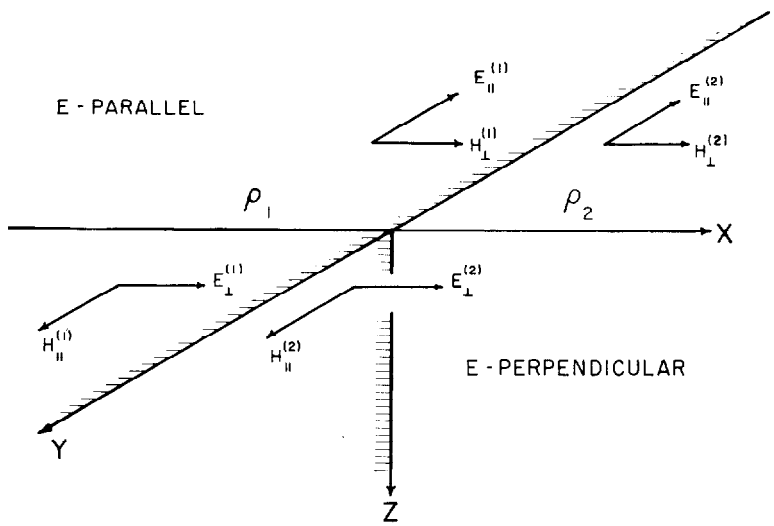

FIG. 1. Electromagnetic field components for $E_\parallel$ and $E_\perp$ polarization.

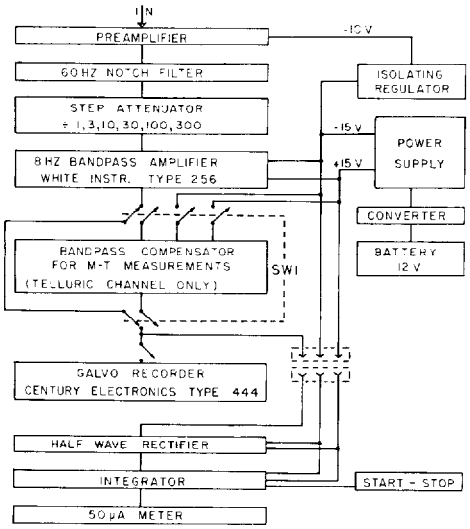

FIG. 2. Block diagram of 8-hz amplifiers.

typical power spectrum of the Schumann resonance magnetic field (Shand, 1966). The sensitivity of the amplifiers is of the order of 1 μv for 3 db signal-to-noise ratio. Power is supplied by two 6-v lantern batteries which provide about forty hours of operation. The total weight of each amplifier unit is approximately 8 lb.

An air-cored induction coil, capacitively tuned to 8 hz, was used to detect the magnetic field (Becker, 1967). A Princeton Applied Research CR-4 low-noise amplifier provided an additional gain stage before the 8-hz amplifier. The sensitivity of the magnetic sensing system is about 0.4 milligammas for 3 db signal-to-noise ratio.

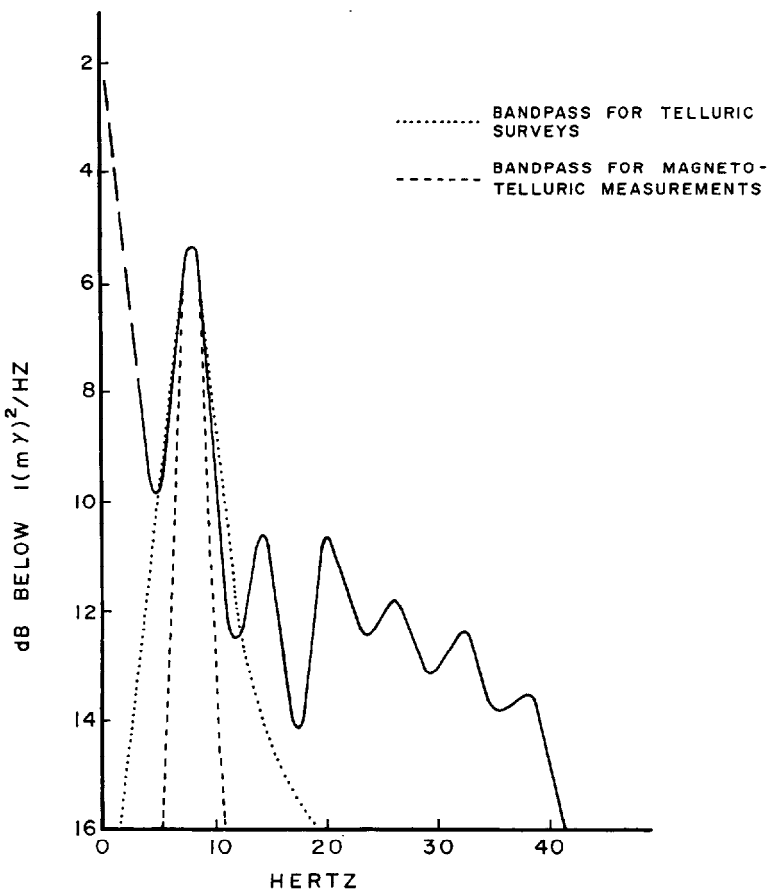

FIG. 3. Power spectrum of subaudio-frequency natural magnetic field (Shand, 1966) and bandpass of telluric and magnetotelluric amplifiers.

FIELD PROCEDURE

Telluric surveys were carried out by establishing a fixed base station, moving the field station along a traverse line, and either recording or integrating the two signals simultaneously. For recording purposes the output of the field amplifier was transmitted through a two-wire cable to the recorder located at the base station. In general, however, only the average value of the signals was desired; the connecting cable was unnecessary. Using a portable transceiver, the base station operator gave the signal to start integration and both operators used stop watches to time the 30-sec integration period. At each field-station location, the integrations were repeated three or more times to obtain a reasonable average value for the relative telluric field strength. Figures 4(a) and 4(b) show the equipment layout for measuring the telluric field perpendicular and parallel to the strike of a conductive zone.

The normal production rate was about 15 stations per hour or an average of two miles per day of continuous profiling with a station spacing of 100 ft.

Magnetotelluric surveys were initially carried out by measuring the telluric field along the traverse line and the horizontal magnetic field at right angles to it [Figure 4(c)]. It was hoped that magnetotelluric surveys, which measure the apparent resistivity directly, would be practical and perhaps superior to telluric surveys, since it would not be necessary to maintain a base station to monitor fluctuations of the background signal.

Magnetotelluric measurements proved to be extremely slow compared to telluric surveys, partly because of the extra equipment involved. However, the main disadvantage was due to the sensitivity of the induction coil to wind-induced ground motion. Any movement of the coil through the earth's magnetic field produced a large 8-hz signal, because of the tight tuning. Consequently, reliable magnetic field measurements were possible only in very calm weather, usually at night.

Another factor also made the magnetic field measurement unimportant. Telluric traverses could be made conveniently only along cut lines, which are generally oriented approximately normal to the strike of the target zone—that is, the $E_\perp$ field direction. As mentioned previously, for this polarization all the significant resistivity information should be contained in variations of the telluric field strength. For these reasons magnetotelluric measurements were made only occasionally.

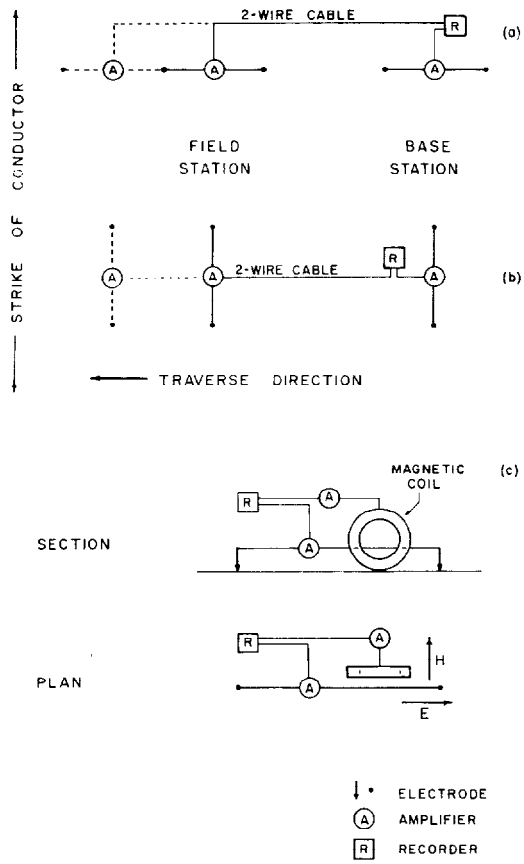

FIG. 4. Equipment layout for field measurements: (a) Telluric field perpendicular to strike ($E_\perp$). (b) Telluric field parallel to strike ($E_\parallel$). (c) Magnetotelluric measurements.

Initial field tests (Slankis and Becker, 1969; Slankis, 1970) were designed to determine the optimum survey methods and to establish the reliability and repeatability of measurements. Massive near-surface sulfide zones, which could be expected to show well-defined anomalies, were chosen for the first field tests. From these trials it was clear that measurements of the telluric field strength normal to the strike of the target zone, combined with spot magnetotelluric determinations of the background apparent resistivity, provided maximum information in relation to the

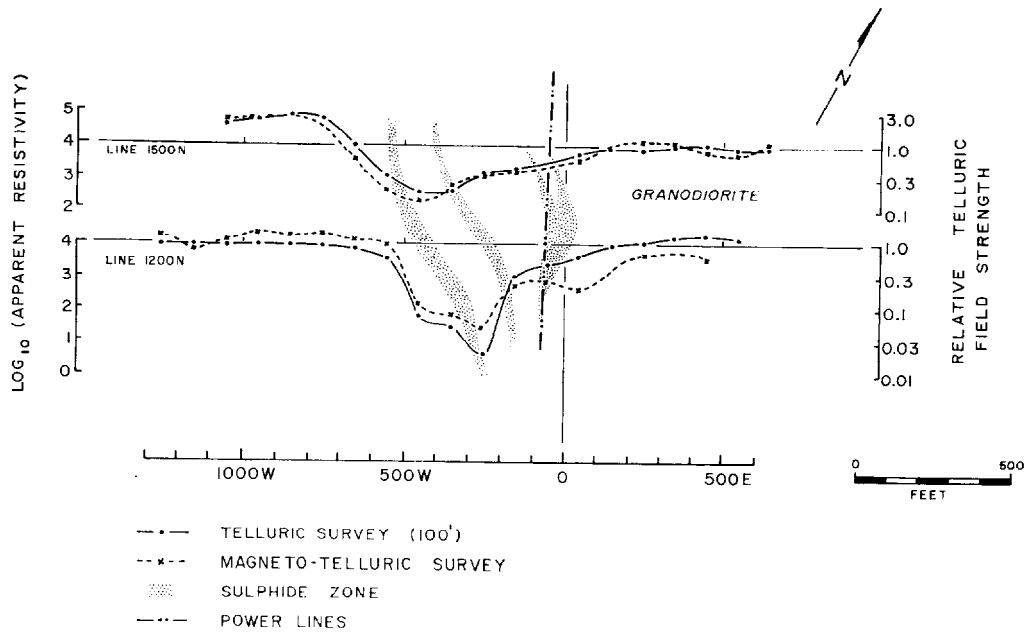

FIG. 5. Test site 1. Telluric and magnetotelluric survey results over northern part of the test site ($E_\perp$ polarization).

work involved. Subsequent test sites were selected to examine the usefulness of the methods in a variety of geologic situations.

FIELD RESULTS AND INTERPRETATION

The results obtained using the various measurement techniques are illustrated by four typical field cases. For the $E_\perp$ polarization the field results are compared with profiles obtained from theoretical models. In most instances, there was sufficient drill-log information to model the geology with relatively good accuracy. The overburden thickness is derived from hammer seismic measurements (Scott, 1970).

The resistivity of the host rocks assumed for the model is the background apparent resistivity obtained from magnetotelluric measurements. Overburden resistivity is taken to be 500 ohm-m if the test site is well drained and 100 ohm-m if the ground is swampy. Resistivity of the sulfide zones ranges from 0.1 ohm-m for very massive sulfides to 20 ohm-m for disseminated mineralization.

For simplicity, the theoretical models are assumed to be structures with well-defined boundaries, where the resistivity changes abruptly. This approach ignores gradual resistivity changes that may be caused by thin sulfide veins and haloes of disseminated mineralization frequently found on the periphery of sulfide zones. However, in cases involving closely spaced parallel or subparallel sulfide bodies, such sporadic mineralization may form an electrical connection between the main zones. This situation is approximated in the theoretical models by joining the zones with a thin conductive layer whose depth is too great to produce a significant anomaly of its own.

Test site 1

This field survey was carried out over a series of steeply dipping massive sulfide bodies. Only the main zones are outlined by diamond drilling. Many drill holes show additional narrow sulfide intersections, but the information available is not sufficient to delineate them. The sulfide content averages 50–60 percent for most zones. There are high-tension power lines and shallowly buried water pipes along the base line. Figures 5 and 6 show a plan of the geology and summarize the field results over the northern and southern parts of the test area.

The telluric and magnetotelluric profiles show similar intense anomalies over the sulfide zones

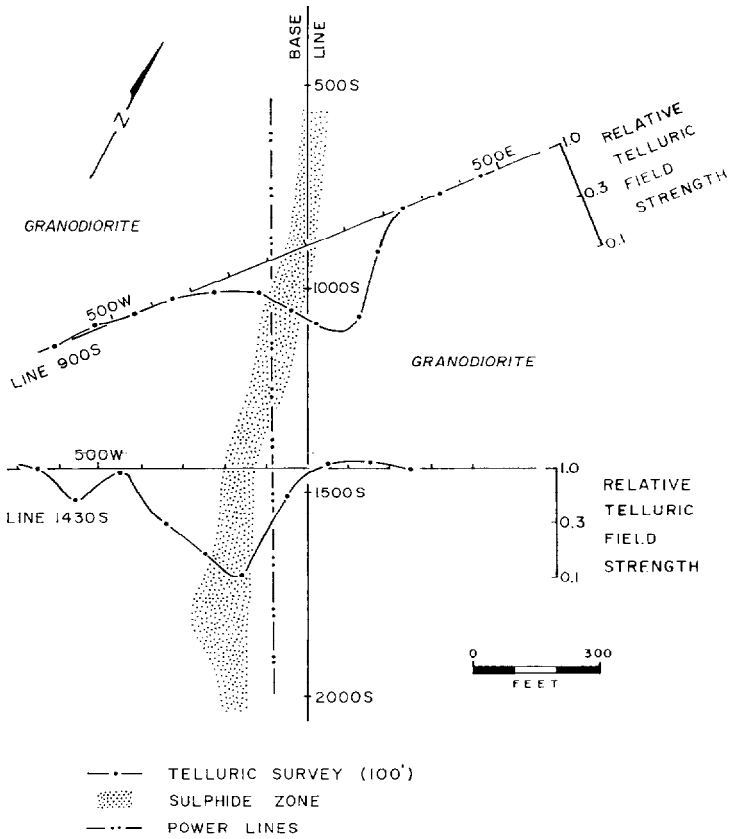

FIG. 6. Test site 1. Results of telluric surveys in southern part of the test site ($E_\perp$ polarization).

(Figure 5). The telluric field strength decreases by a factor of more than 30, and the minimum apparent resistivity is less than 30 ohm-m compared to the background value of 10,000 to 20,000 ohm-m. The agreement between telluric and magnetotelluric results is good.

The power line did not affect the survey when the telluric field was measured normal to it; but close to the line the parallel telluric field was very large, and its appearance did not resemble that of the usual 8-hz signal. This situation was somewhat unusual because, generally, 60-hz noise did not pose a problem regardless of the direction of measurement.

The theoretical telluric field strength profile for line 1200N shows some similarity to the observed field strength (Figure 7). The greater width of the observed anomaly probably results from the fact that the traverse crosses two of the sulfide zones at an oblique angle. On line 900S the agreement between the theoretical and observed profiles is poor. Unfortunately, only one drill hole exists in the area of this traverse so that the geologic section may be incomplete. The field results suggest the presence of a much wider conductive zone than outlined by the drilling, or, as on line 1200N, the observed anomaly may be affected by the fact that the telluric field was not measured normal to the strike.

Test site 2

The mineralization at this test site consists of several parallel sulfide lenses located in a shear zone near a contact between volcanic and sedimentary rocks (Figure 8). The location of the sulfide zones is based on diamond drill data and on a

horizontal-loop EM survey. The sulfide content ranges from massive to disseminated; considerable mineralization exists between the main zones.

Except for better detail over the anomalous zones, the profiles obtained using 25-ft electrode spacing are very similar to those from the 100-ft surveys. Because telluric measurements sample an existing electric field strength pattern, the electrode separation does not affect the depth of penetration. The use of long spreads does, however, reduce the resolution as anomalies are smoothed out; for very large spreads they may disappear completely.

West of the mineralized zones the telluric field strength is relatively constant with no indication of the geologic contact. To the east the small variations in the field strength suggest the presence of additional weakly conductive zones.

Figure 9 shows the telluric field strength profiles for the $E_{\parallel}$ polarization. The presence of the sulfide mineralization is indicated, but the anomalies are not as well defined as in the $E_{\perp}$ case.

The results of horizontal loop surveys (Figure 10) clearly show the presence of the massive sulfide zone but give little indication of the disseminated zones which contain 5–35 percent sulfides.

Figure 11 compares theoretical and observed telluric profiles along three lines where the geology

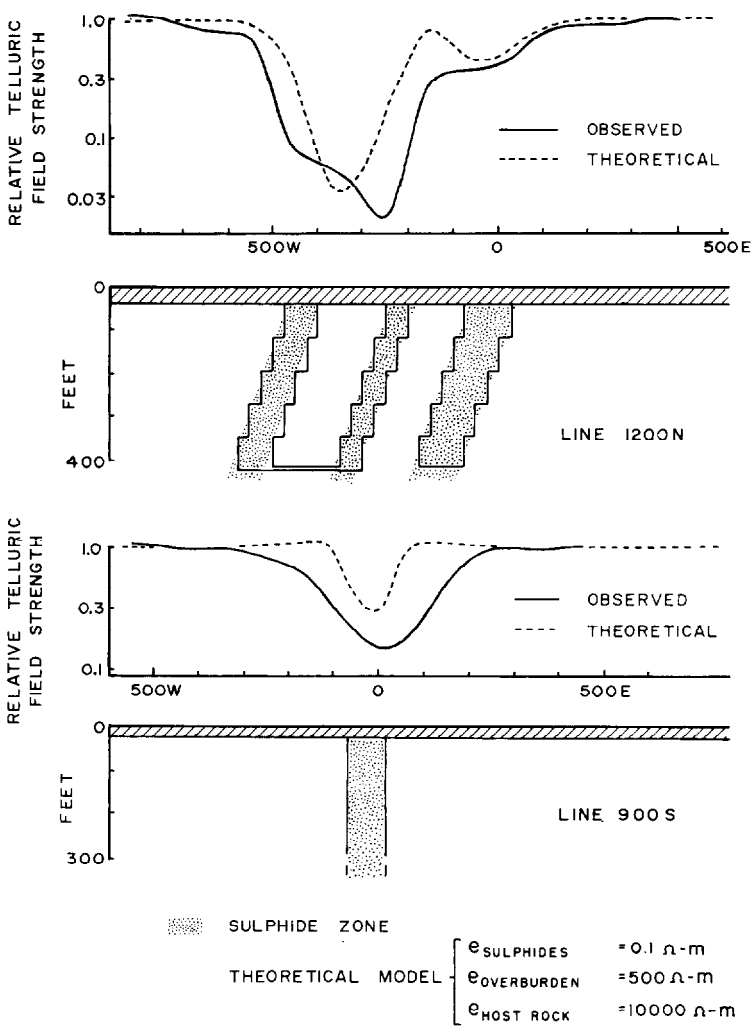

FIG. 7. Test site 1. Observed and theoretical telluric profiles ($E_{\perp}$ polarization).

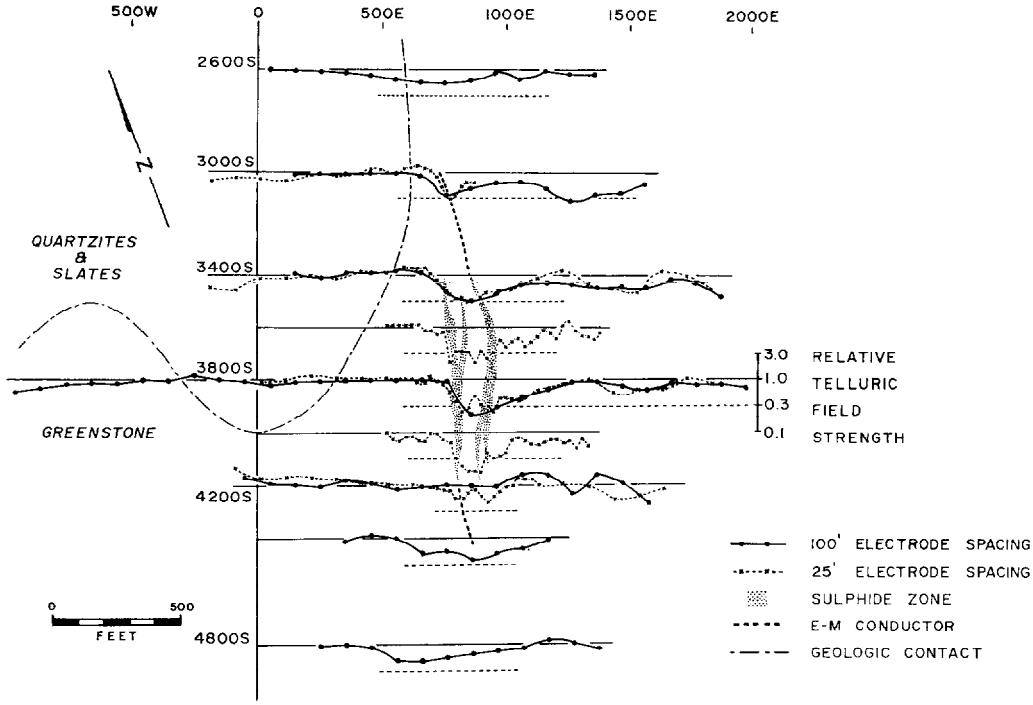

FIG. 8. Test site 2. Results of telluric surveys ($E_{\perp}$ polarization).

is relatively well known. On line 3800S the drill holes do not reach the sulfide zones between 925E and 950E; their location is based on drill results on the adjacent lines. The theoretical and observed anomalies over the known mineralized zones are comparable in their shape and magnitude provided that the zones are electrically connected in the model.

Test site 3

This location was selected because of the availability of results from Turam, induced-polarization, horizontal-loop, and magnetic surveys (Lavoie, 1968).

The mineralization consists of two parallel sulfide bodies, containing 10–40 percent total sulfides, located at the contact between acidic flows and rhyolite porphyry. The area is covered by muskeg.

Telluric surveys (Figure 12) show no anomaly over the sulfides but seem to indicate the geologic contact. Of the other geophysical methods, only the magnetic survey shows an anomaly over the sulfide zones.

The theoretical results (Figure 13) suggest that the observed telluric profile mainly reflects variations in the overburden thickness rather than different resistivities on opposite sides of the contact.

Test site 4

The mineralization at this site consists of a large body of massive sulfides located in diorite-rhyolite host rock. The zone subcrops below thin overburden in the south and plunges gently to a depth of 400 ft at the north end.

The low signal levels within 200 to 300 ft of the sulfide zone necessitated the use of 100-ft electrode spreads. In addition to the telluric measurements, a number of magnetotelluric determinations were made in order to evaluate the background resistivity.

The survey results, presented in the form of a resistivity map (Figure 14), clearly indicate the presence of the sulfide zone. The apparent resistivity is lowest in the south and where the zone is near surface. To the north, the last definite indication is on line 1930S where the zone is more than 200-ft deep.

Figure 15 compares theoretical and observed

profiles along lines 2630S, 2330S, and 1930S. There is fair agreement between the two profiles on lines 2330S and 2630S, but on line 1930S the field results suggest that the middle of the sulfide zone is deeper than the sides.

GENERAL THEORETICAL CONSIDERATIONS

Some numerical experiments with the computation method showed it to be accurate to about 3 percent. This figure was obtained by comparing the numerical data with the analytical results of D'Erceville and Kunetz (1962).

For the $E_{\perp}$ polarization, theoretical profiles are in general agreement with field results. For this polarization, therefore, the conclusions derived from a study of a generalized theoretical model can be extended to actual field situations.

The model considered is a tabular body of 50-ohm-m resistivity buried in a 5000-ohm-m medium. The basic body has a width of 100 ft, a depth of burial of 50 ft, and a depth extent of 200 ft. The theoretical anomalies are calculated for a source field frequency of 8 hz.

Increasing the resistivity contrast [Figure 16(a)] intensifies the anomaly. In this particular model a limit is reached at a contrast of 50; greater contrasts have essentially no effect on the profile. The limiting value depends on the geometry of the model and will be larger than 50 if the width-to-depth ratio of the conductor increases.

The most important factor in determining the intensity of the anomaly is the width-to-depth ratio of the conductive zone [Figure 16(b) and (c)]. The geometric nature of this effect can be seen in the similar values for the minimum apparent resistivity obtained for corresponding width-to-depth ratios in the two figures. In Figure 16(c) the minimum apparent resistivity over the 500-ft-wide body is a limiting case; little change in contrast is observed for larger values of W, although clearly the profile becomes wider.

Changes in the depth extent [Figure 16(d)] affect the profiles much less than variations in any other parameter.

The cross-sectional area of the conductive zone has been maintained constant for the dipping slabs shown in Figure 17(a). As the dip decreases the profile becomes increasingly asymmetric, while the peak on the updip side becomes progressively greater than the background value. On the downdip side the profile remains smooth. The increase in anomaly intensity and width with decreasing dip can be attributed to the larger effective width-to-depth ratio of the conductor.

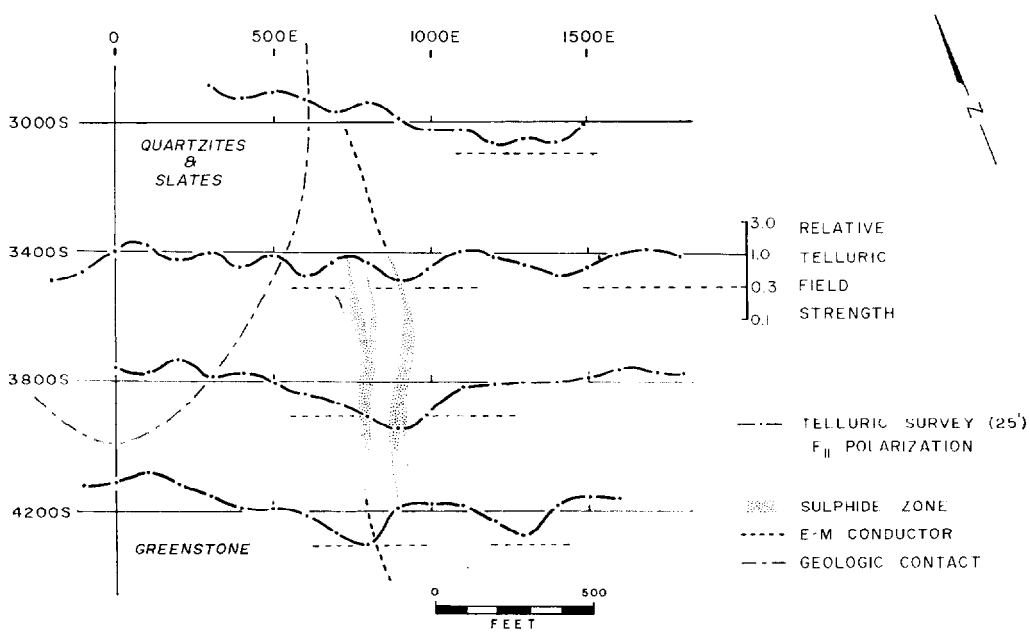

FIG. 9. Test site 2. Results of telluric surveys ($E_{\parallel}$ polarization).

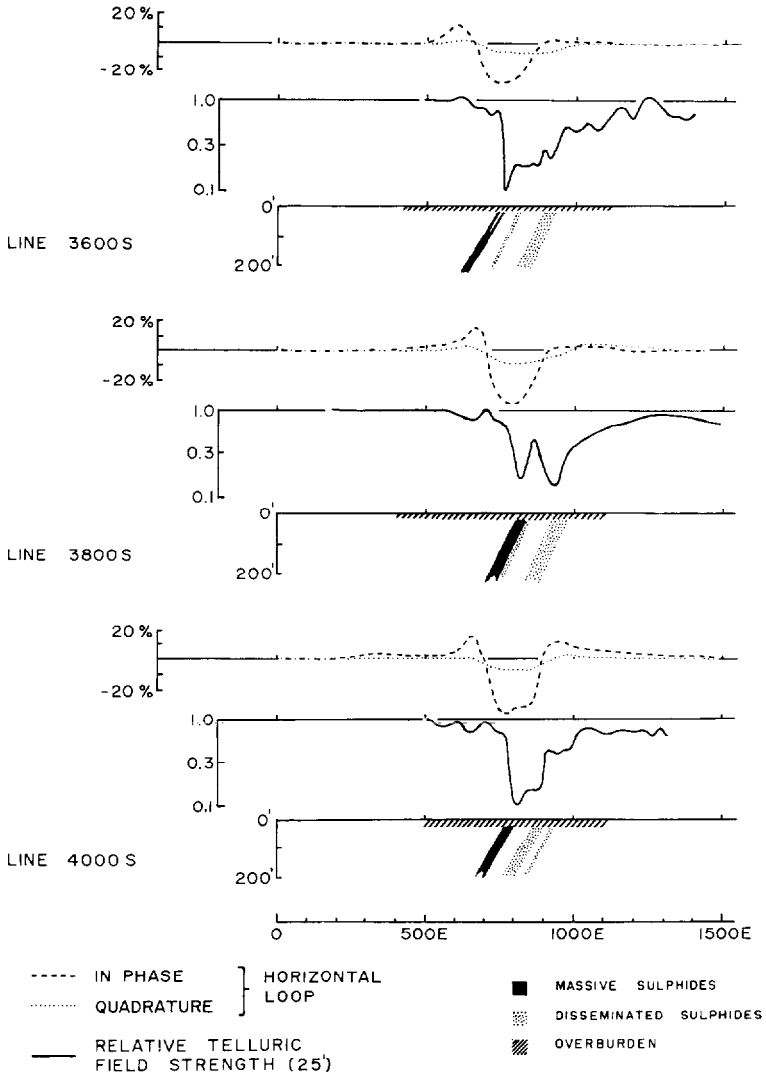

FIG. 10. Test site 2. Comparison of horizontal loop and telluric ($E_\perp$) survey results.

The effect of conductive overburden [Figures 17(b), (c), and (d)] depends primarily on the resistivity contrast between the overburden and the conductive zone. For contrasts greater than 5, the change in the relative telluric field strength decreases by less than 15 percent from that observed with no overburden-bedrock contrast.

For larger width-to-depth ratios, the overburden effect is more pronounced, but, on the other hand, the anomaly is also more intense. In these diagrams the apparent resistivity is not shown in order to permit stacking of the profiles. The background apparent resistivity varies from 5000 ohm-m with no overburden contrast to 1700 ohm-m for an overburden resistivity of 10 ohm-m.

No theoretical results are presented for the $E_\parallel$ polarization because there was no agreement between the theoretical and observed profiles. At 8 hz the theoretical telluric $E_\parallel$ field decreases only slightly over models of conductive zones where the observed field shows a strong anomaly. The discrepancy arises from the necessity of using

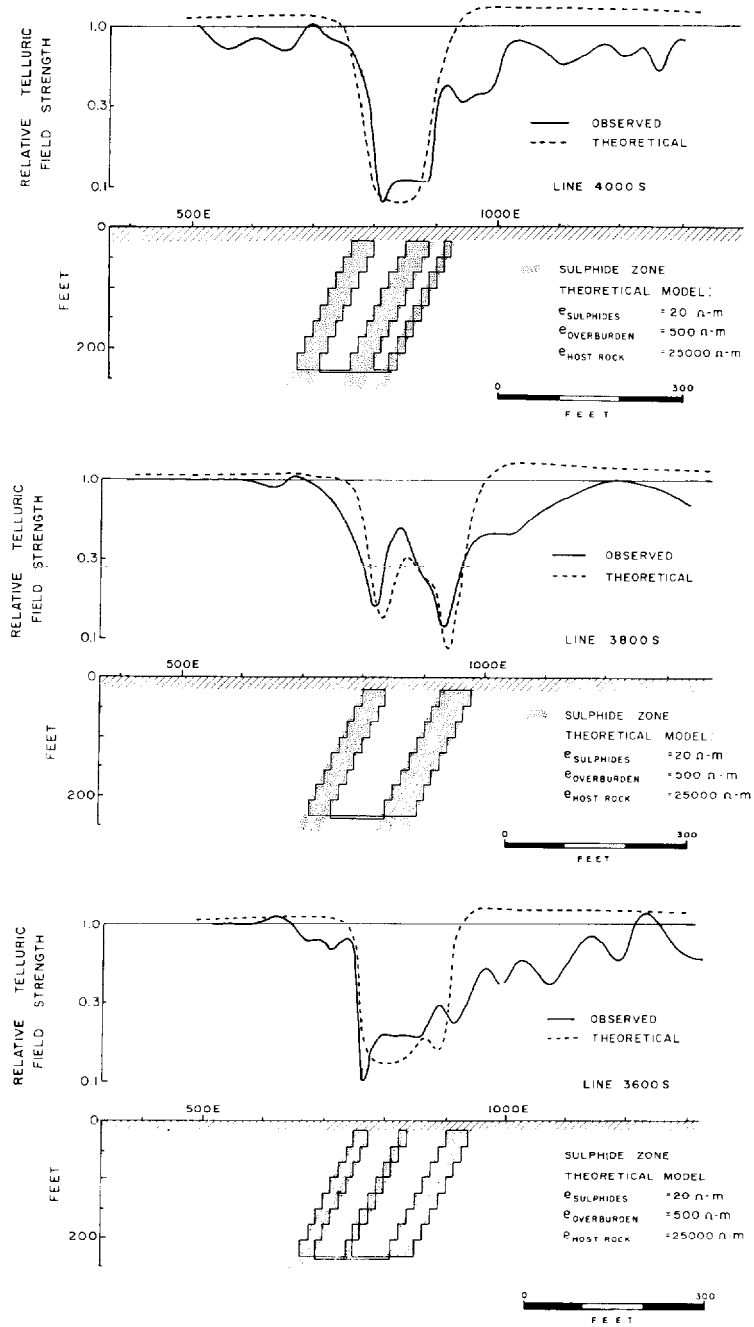

FIG. 11. Test site 2. Observed and theoretical telluric profiles ($E_{\perp}$ polarization, 25-ft electrode spacing).

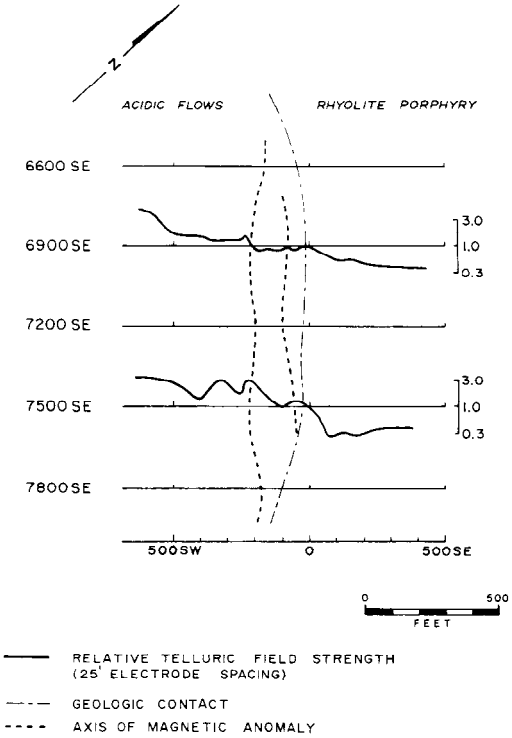

FIG. 12. Test site 3. Results of telluric surveys ($E_\perp$ polarization).

two-dimensional models of infinite strike extent for actual three-dimensional conductivity structures of limited strike length.

This can be explained qualitatively by considering the behavior of the electromagnetic field components at the ends of a conductive rectangular slab buried in a resistive medium. In the $E_\parallel$ case the observed anomaly is affected by limited strike length because the amplitude of the electric field and the normal derivatives of the associated magnetic field components are discontinuous across the ends of the slab. Thus, unless the conductor is very long compared to the skin depth at the frequency of measurement, the two-dimensional model is not appropriate. Conversely, in the $E_\perp$ case, all the electromagnetic field components are continuous across the ends of the slab so that strike length should not significantly affect the observed anomaly. Practically, if the length-to-width ratio of the conductor is greater than four, the two-dimensional approximation seems to be valid.

This restriction on the use of the two-dimensional models for the $E_\parallel$ polarization becomes less important at higher frequencies. For AFMAG and, especially, VLF analysis (Vozoff, 1971), theoretical results should be applicable to most of the conductivity features encountered in the field.

DISCUSSION AND CONCLUSIONS

Both telluric and magnetotelluric surveys can detect conductivity anomalies associated with some mineralized zones. In cases where results

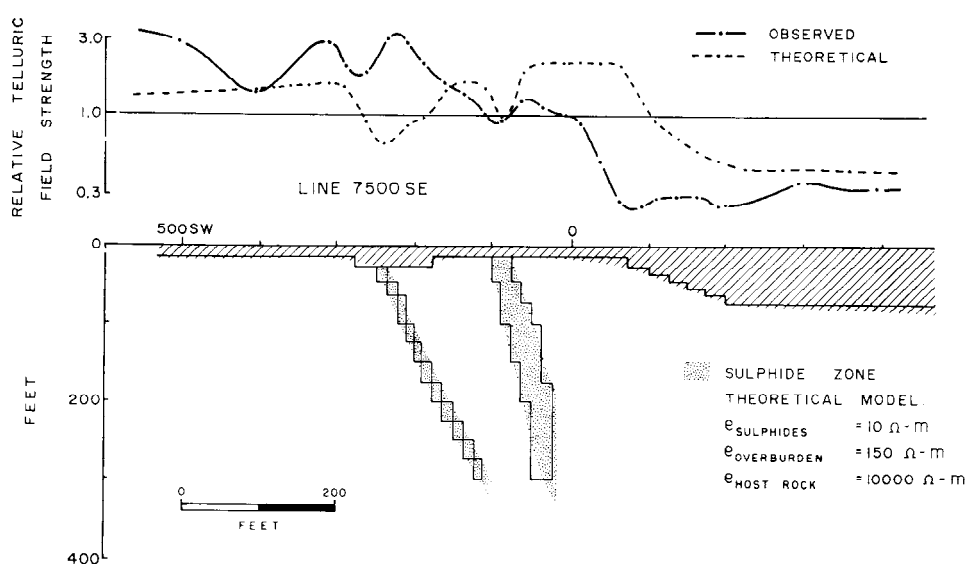

FIG. 13. Test site 3, Line 7500 SE. Observed and theoretical telluric profiles ($E_\perp$ polarization).

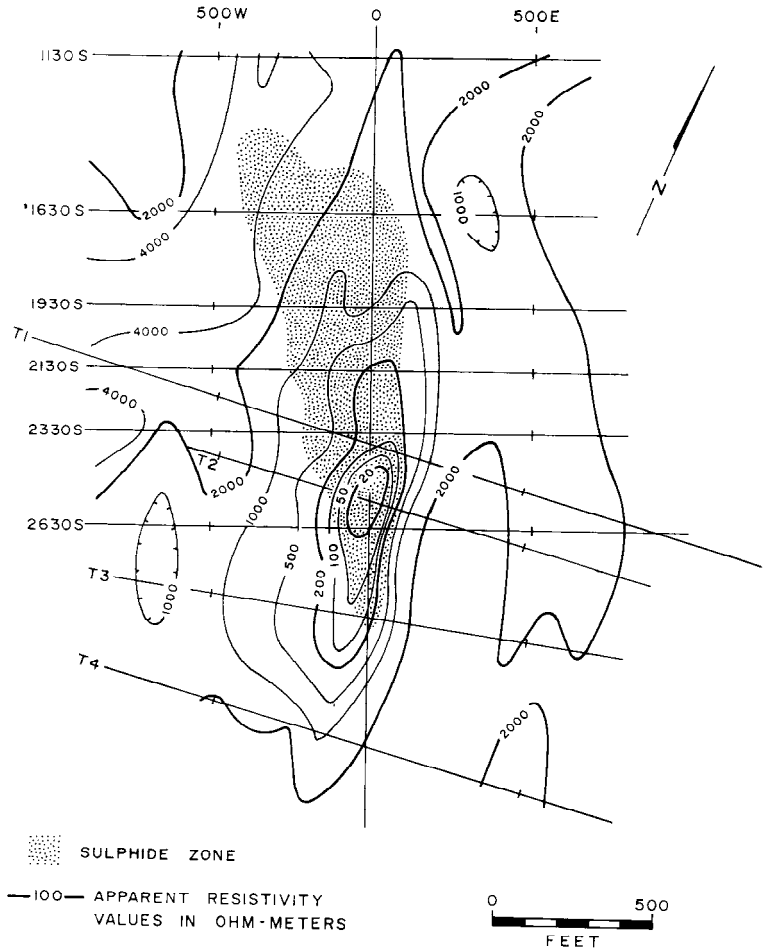

FIG. 14. Test site 4. Apparent resistivity map based on results of relative telluric field strength measurements ($E_\perp$ polarization).

from other methods are available for comparison, the penetration and resolution of the natural field surveys are generally comparable to those of standard electrical and electromagnetic geophysical techniques.

For the $E_\perp$ polarization, magnetotelluric determinations of apparent resistivity and relative telluric field strength measurements give equivalent results as predicted by magnetotelluric theory. As discussed previously, the telluric method is superior to the magnetotelluric in terms of survey speed, equipment requirements, repeatability of results, and the absence of wind-noise problems. Thus, there is no advantage in obtaining unidirectional absolute values of apparent resistivity by magnetotellurics over the calculation of relative values of this quantity as obtained from tellurics alone.

The best results are achieved by measuring the telluric field normal to the strike of the target zone. The anomalies observed are more intense and better defined than those for the parallel telluric field. However, since anomalies are observed for both polarizations, the method will detect conductive zones regardless of the survey direction.

The depth penetration of the telluric method is limited primarily by the fluctuations in background field strength (i.e., geologic noise) and the width-to-depth ratio of the target zone. As the

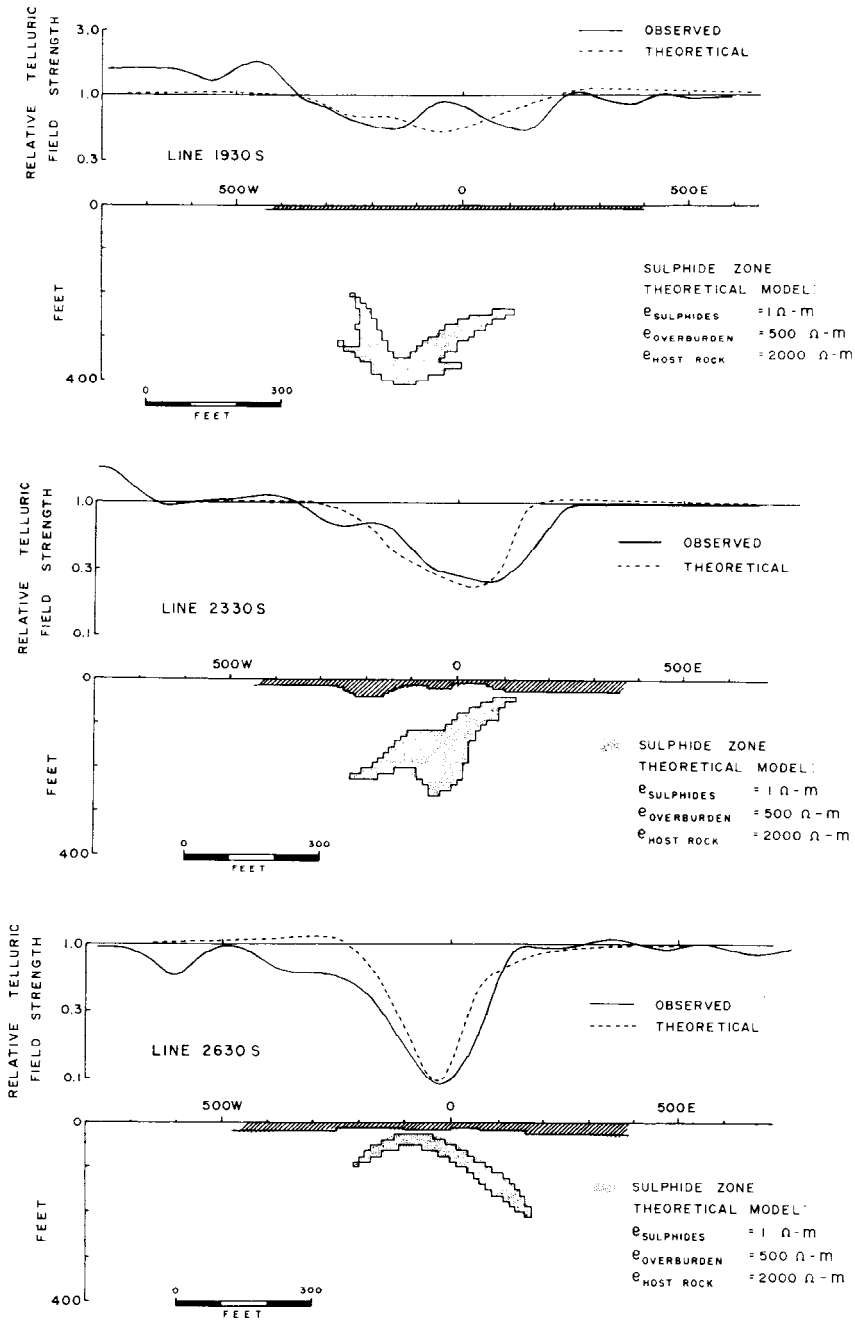

FIG. 15. Test site 4. Observed and theoretical telluric profiles ($E_{\perp}$ polarization).

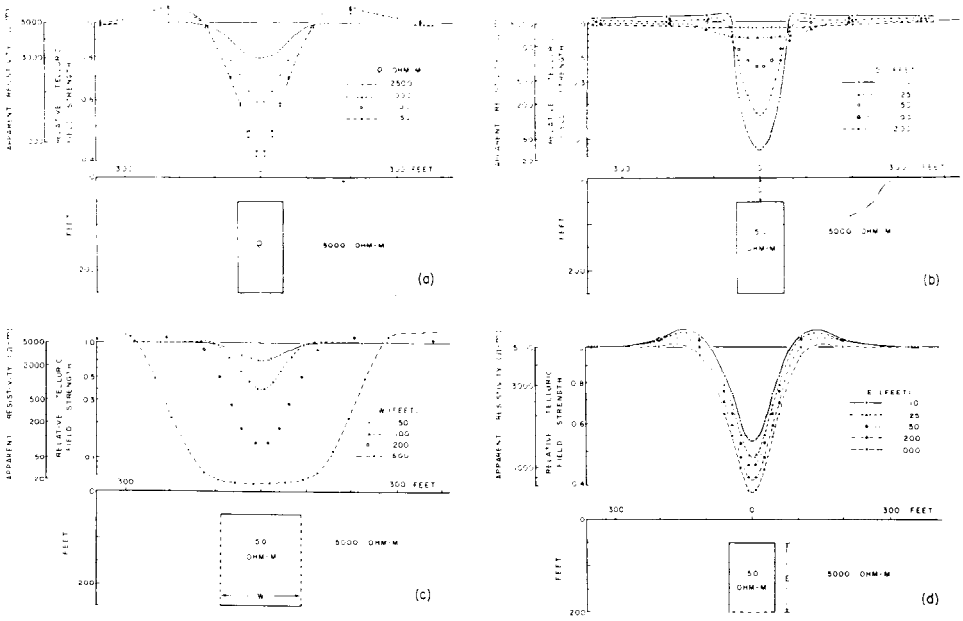

FIG. 16. Theoretical effects of dike resistivity and geometry ($E_\perp$ polarization).

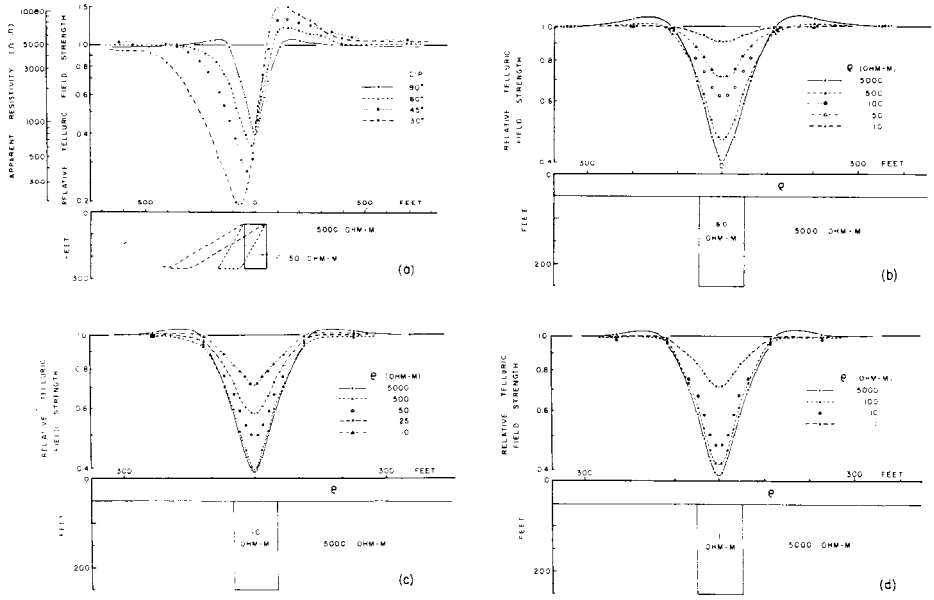

FIG. 17. Theoretical effects of dike inclination and overburden resistivity ($E_\perp$ polarization).

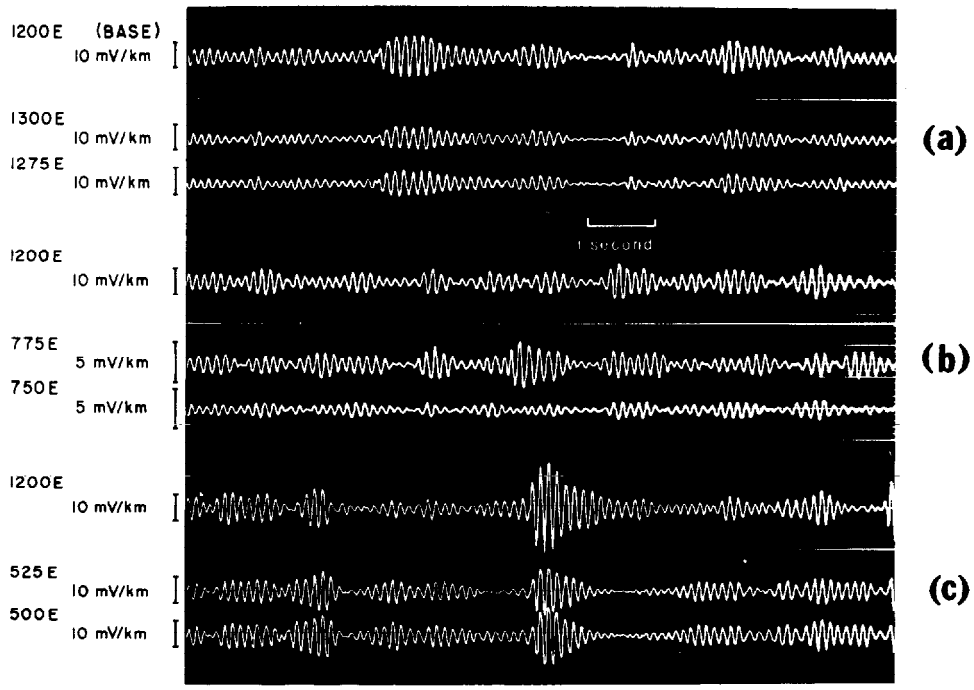

FIG. 18. Test site 2, Line 3600S. Comparison of telluric signals.

background field at some locations may vary by 50 percent, there is good reason to ignore anomalies where the field strength does not decrease to at least 0.3 of the background value. On the basis of Figure 17(b), such a change would be equivalent to a minimum width-to-depth ratio of 3 for a conductive dike. Thus, the method is not particularly useful for detection of narrow and steeply dipping conductors but shows considerably more sensitivity to flat-lying sheets or wide dikes. The response of multiple conductive zones is unpredictable and seems to depend entirely on whether the zones are electrically connected.

The method appears to have good potential for penetrating conductive overburden but, as illustrated by the results at test site 3, is susceptible to rapid lateral changes in the overburden thickness.

Interpretation of field results is highly qualitative. Generally, the width of the anomaly corresponds fairly closely to the conductor width, but, in many instances, fluctuations in the background field on the flanks of an anomaly make width determinations difficult. This problem may be further complicated by the presence of multiple conductive zones. Similarly, the direction of dip cannot be deduced with any certainty unless the actual dip is less than 45 degrees. Estimates of the maximum possible depth of burial can be made from type curves by using the width of the anomaly and the maximum change in the relative telluric field strength to determine the width-to-depth ratio and, hence, the depth of the anomaly source.

One peculiar feature, observed at test sites 2 and 4, merits some discussion. Figure 18 illustrates changes in the telluric signals at the base and field stations during the survey along line 3600S at site 2. These results are typical of the behavior of the telluric field in the vicinity of a highly conductive shallow zone. When the base and field stations are on the same side of the conductive zones [Figure 18(a)] the signals are in phase and correlate well. The presence of the conductive sulfides is, of course, indicated by a decrease in the amplitude of the field-station signal. Also, the base- and field-station signals are not coherent [Figure 18(b)]. When the stations are on opposite sides of the conductor [Figure 18(c)], the

signals are again in phase and correlate fairly well.

A similar loss of correlation was observed within 200 to 300 ft of the sulfide zone at test site 4. This effect, coupled with a sudden large phase shift, occurred during several additional field surveys in which base- and field-station signals were recorded and also has been reported by others. Nor do the theoretical calculations offer any explanation for the observed change in phase and correlation; the phase of the theoretical telluric fields over the sulfide zones differs by less than 20 degrees from that of the background field. Certainly this anomalous behavior requires further study.

REFERENCES

Becker, A., 1967, Design formulas for electromagnetic sensing coils: Geoexploration, v. 5, p. 81–88.

Berdichevskiy, M. N., 1960, Electrical prospecting with the telluric current method: Moscow, Gostoptekhizdat, Eng. Trans., Keller, G. V., 1965, Quart. Colo. School of Mines, v. 60, no. 1.

Boissonnas, E., and Leonardon, E. G., 1948, Geophysical exploration by telluric currents, with special reference to a survey of the Haynesville salt dome, Wood County, Texas: Geophysics, v. 13, p. 387–403.

Cagniard, L., 1953, Basic theory of the magnetotelluric method of geophysical prospecting: Geophysics, v. 18, p. 605–635.

Collett, L. S., and Bell, C. K., 1971, The use of AFMAG in geological interpretation: CIM Bull., v. 64, no. 706, p. 39–47.

Dahlberg, R. S., Jr., 1945, An investigation of natural earth currents: Geophysics, v. 10, p. 494–506.

D'Erceville, I., and Kunetz, G., 1962, Effect of a fault on the earth's natural electromagnetic field: Geophysics, v. 27, p. 651–665.

Galejs, J., 1964, Terrestrial extreme-10w-frequency propagation, *in* Natural electromagnetic phenomena below 30 Kc/s: D. F. Bleil, editor, New York, Plenum Press, p. 205–260.

Lavoie, C., 1968, Etude geophysique de trois gisements de sulfures sous des morts-terrains epais et conducteurs: Department de Genie Geologique, Ecole Polytechnique de Montreal, Montreal, Canada, M.Sc thesis.

Madden, T. R., and Swift, C. M., Jr., 1969, Magnetotelluric studies of the electrical conductivity structure of the crust and upper mantle, *in* The earth's crust and upper mantle: P. J. Hart, editor, Geophys. Monogr. 13, Amer. Geophys. Union, p. 469–479.

Madden, T. R., and Thompson, W., 1965, Low frequency electromagnetic oscillations of the earth-ionosphere cavity: Rev. Geophys., v. 3, no. 2, p. 211–254.

Neuenschwander, E. F., and Metcalf, D. F., 1942, A study of electrical earth noise: Geophysics, v. 7, p. 69–77.

Scott, W. J., 1970, Private communication.

Shand, J. A., 1966, Some quantitative characteristics of the Schumann-ELF natural electromagnetic background: Can. J. Phys., v. 44, no. 3, p. 449–459.

Slankis, J. A., 1970, Telluric and magnetotelluric surveys at 8 hz: McGill University, Montreal, Canada, Ph.D. thesis, 136 p.

Slankis, J. A., and Becker, A., 1969, Telluric and magnetotelluric measurements at 8 hz: AIME Trans., v. 244, p. 237–244.

Srivastava, S. P., Douglass, J. L., and Ward, S. H., 1963, The application of magnetotelluric and telluric methods in Central Alberta: Geophysics, v. 28, no. 3, p. 426–446.

Strangway, D. S., and Vozoff, K., 1970, Mining exploration with natural electromagnetic fields: Mining and Groundwater Geophys., 1967, Geol. Surv. Can., Econ. Geol. Rep., no. 26, p. 109–122.

Swift, C. M., Jr., 1971, Theoretical magnetotelluric and Turam response for two-dimensional inhomogeneities: Geophysics, v. 36, no. 1, p. 38–52.

Vozoff, K., 1971, The effect of overburden on vertical component anomalies in AFMAG and VLF exploration: A computer model study: Geophysics, v. 36, no. 1, p. 53–57.

Weaver, J. T., 1963, The electromagnetic field within a discontinuous conductor with reference to geomagnetic micropulsations near a coast line: Can. J. Phys., v. 41, p. 484–495.